energy&fuels

pubs.acs.org/EF Article

Co-processing of Hydrothermal Liquefaction Biocrude with Vacuum Gas Oil through Hydrotreating and Hydrocracking to Produce Low-Carbon Fuels

Sandeep Badoga, Anton Alvarez-Majmutov,* Tingyong Xing, Rafal Gieleciak, and Jinwen Chen

Cite This: *Energy Fuels* 2020, 34, 7160–7169

Read Online

ACCESS | Metrics & More | Article Recommendations

ABSTRACT: In this study, we investigate the potential of co-processing hydrothermal liquefaction (HTL) biocrude with vacuum gas oil (VGO) in a hydrocracking process with hydrotreating as the first step. Experiments were conducted in a continuous hydroprocessing pilot plant in two stages: hydrotreating and hydrocracking. Two feeds were tested: first pure VGO to establish a baseline and then a co-processing blend having 7.5 vol % HTL biocrude. In the first stage, the VGO and co-processing blend were sequentially hydrotreated to meet the quality specification of the hydrocracking catalyst. The second stage consisted of hydrocracking the two hydrotreated products from the first stage, and the resulting products were distilled into naphtha, diesel, and jet fuel fractions for characterization. The hydrotreating step achieved satisfactory sulfur and nitrogen removal levels for both feeds, but it was ineffective in converting oxygen compounds in the co-processing blend, resulting in a product with 1530 ppmw oxygen. During hydrocracking, the co-processing blend required a higher reaction temperature than the baseline VGO to achieve the same conversion level, a behavior attributed to the oxygen and nitrogen levels in the co-processing blend after hydrotreating. Despite these effects, overall product distribution and hydrogen consumption for both scenarios were quite comparable. Characterization of hydrocracked products showed only subtle differences in quality and hydrocarbon type composition, while biogenic carbon measurements revealed that the majority of biogenic carbon is transferred to the naphtha, diesel, and jet fuel fractions.

1. INTRODUCTION

Increasing the consumption of low-carbon transportation fuels is becoming essential to reduce the climate change impact of the transportation sector. A number of countries are already blending ethanol into petroleum gasoline and biodiesel into petroleum diesel in ratios of up to 20 vol %.[1,2] Canadian federal regulations mandate a minimum renewable content of 5 vol % in gasoline and 2 vol % in diesel fuels that are either produced in or imported into Canada.[3] With the introduction of low-carbon-fuel standards as a means to enact carbon intensity reduction of transportation fuels, the growing demand for biofuels is creating the need for additional biofuel technology options that utilize unconventional biomass resources, such as forest residues, agricultural wastes, algae, sewage sludge, and organic municipal solid waste. Pyrolysis,[4−6] hydrothermal liquefaction (HTL),[7,8] and thermocatalytic reforming (TCR)[8−10] are among the technologies that can take this type of biomass and convert it into a liquid product intermediate, known as bio-oil or biocrude, that can be further upgraded into biofuels in a stand-alone biorefining process or by co-processing in a petroleum refinery. The latter option has a cost advantage, as most of the infrastructure and utilities required for co-processing are already in place in the refinery.

Extensive literature reviews[11−15] discussing diverse scenarios for integrating biogenic feedstocks into refineries show that significant progress has been made in co-processing vegetable oils in fluid catalytic cracking (FCC) and hydroprocessing units. In fact, several refineries in North America and Europe have been conducting commercial trials using lipid feedstocks, such as canola oil, rapeseed oil, sunflower oil, tall oil, and animal fats.[16−19] The strategy to co-process biocrudes or bio-oils in a petroleum refining scheme remains an open question owing to the unique character of each biocrude, which is imparted by the pairing of a waste biomass feedstock with a specific thermochemical conversion technology. Considerable efforts[20−22] have been devoted to utilizing fast pyrolysis bio-oils as co-processing feed in FCC units encountering, in most cases, difficulties related to catalyst underperformance as a result of the elevated oxygen content (up to 40 wt %) in these bio-oils. A number of studies[23−26] concur that partial hydrodeoxygenation (HDO) is essential to making pyrolysis bio-oils suitable for co-processing, yet HDO has its own technical challenges. Several reviews on bio-oil HDO development[27−29] have pointed out the resistance of HDO catalysts to deactivation by bio-oil compounds as one of the key areas needing improvement to advance this technology.

From the above-cited literature, one can infer that high levels of oxygen in biocrude are a major barrier to co-processing. HTL technologies hold promise in this respect,[30]

Received: March 25, 2020
Revised: May 13, 2020
Published: May 26, 2020

given their ability to produce biocrude with much lower oxygen content (below 15 wt % oxygen)[31] and better chemical stability than pyrolysis bio-oils.[28] However, little has been explored about HTL biocrude utilization in a refinery, in part because this group of technologies is still in development status. Studies by Hoffmann et al.[30] and Jensen et al.[32] discussed potential locations in a refinery to drop in HTL biocrude on the basis of its chemical properties. The authors reached the conclusion that, despite its reduced oxygen content, HTL biocrude still requires some level of oxygen removal to reduce corrosion effects in refinery units. A similar recommendation was put forward in another study[33] attempting to address the miscibility aspect of HTL biocrude with refinery streams. The potential of co-processing HTL biocrude with vacuum gas oil (VGO) in FCC units was investigated by Mathieu et al.[34] Considering that the HTL biocrude sample underwent distillation to prevent heavy components from entering the FCC test unit, there was deterioration of the FCC product yield structure through increased coke and dry gas make at co-processing ratios above 10 wt % biocrude. In the same study, it was shown that lowering the oxygen content in the HTL biocrude via hydrotreating improved performance in the FCC process, allowing higher co-processing ratios. Sauvanaud et al.[35] explored co-processing up to 20 wt % HTL biocrude with petroleum middle distillates in a continuous hydrotreating unit. Co-processing tests with run durations of less than 60 h showed mild changes in product yields and quality. The long-term operational impacts of exposing the hydrotreating catalyst to HTL biocrude were not addressed in their study.

A previous study[36] investigated the potential of co-processing HTL biocrude derived from woody biomass in a VGO hydrotreating process, a scheme through which the oxygen compounds in biocrude would be treated with VGO heteroatoms in preparation for further processing in FCC or hydrocracking units. The proposed scheme was shown to be potentially feasible, provided that the ratio of biocrude in the feed is kept below 10 vol % to reduce the impact on catalyst activity. The next step along this path is to further explore the impacts of co-processing HTL biocrude on the units downstream from the VGO hydrotreater. In particular, co-processing HTL biocrude in a hydrocracker to produce gasoline, diesel, and jet fuel fractions has not yet been studied to the best of our knowledge. Furthermore, the distribution of biogenic carbon across the co-processed fuel products from the hydrocracking process is not well understood. In this paper we seek to address these questions through a detailed pilot testing study.

2. EXPERIMENTAL SECTION

2.1. Feedstock Selection and Preparation. VGO (boiling range of 323−524 °C) distilled from Canadian oil sands bitumen was used as the base petroleum feedstock. Biocrude produced by HTL of woody biomass was made available for this study by Steeper Energy. Before the tests, the biocrude sample was treated to improve its processability. The treatment protocol included filtration to eliminate solid particles that could plug the reactor, followed by distillation under vacuum in an ASTM D-1160 setup to remove any associated water and heavy components boiling above 525 °C. Our early attempts to blend full-range HTL biocrude with VGO resulted in particle agglomeration and deposition, a behavior that was being caused by highly polar oligomeric structures residing in the 525 °C+ fraction of biocrude.[36] While not ideal in terms of yield, separation of this residual fraction became a necessity to manage this incompatibility issue.

The co-processing feedstock, hereafter referred to as biocrude blend, was constituted to be 7.5 vol % HTL biocrude distillate and 92.5 vol % VGO. The biocrude blending ratio was selected to not exceed 10 vol % in order to reduce impacts on the hydroprocessing catalysts[36] while being substantial enough to achieve meaningful biogenic carbon contents in the hydrocracking products.

2.2. Experimental Test Plan. Testing was conducted in a continuous hydroprocessing pilot unit. The experimental test plan consisted of three phases: hydrotreating, hydrocracking, and product fractionation. To create a baseline for the study, testing on pure VGO was included in the experimental plan. In the first phase, the pure VGO and biocrude blend were sequentially hydrotreated over a commercial $NiMo/Al_2O_3$ catalyst to meet the sulfur and nitrogen specifications of the hydrocracking catalyst. Following completion of this phase, the reactor was discharged and then repacked with a commercial bifunctional hydrocracking catalyst to carry out the second phase of the test plan using the two hydrotreated products from the first phase as feedstocks. The hydrocracked liquid products from each feed were distilled to obtain fractions, which were characterized in the third phase. In line with this test plan, a requirement for the pilot plant tests was to generate at the end at least 2 L of hydrocracked liquid product from each feedstock to be able to distill out meaningful quantities of naphtha, diesel, and jet fuel fractions for further analysis. The details of each element of the experimental plan are discussed below.

2.2.1. Hydroprocessing Unit Setup. The hydroprocessing unit comprised a heated feed tank, a pump, gas flow controllers, a tubular reactor (length 105 cm and diameter 0.9 cm) with a heating jacket, high- and low-pressure phase separators, and a gas chromatography (GC) instrument for online gas analysis. Figure 1 shows the reactor packing diagram for the hydroprocessing unit. In each testing phase,

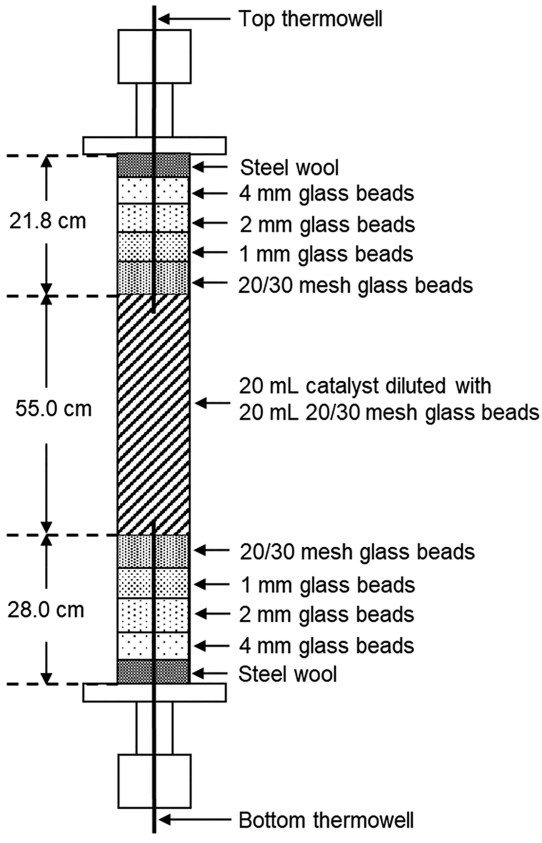

Figure 1. Reactor packing diagram used in this study for hydroprocessing experiments.

https://dx.doi.org/10.1021/acs.energyfuels.0c00937
Energy Fuels 2020, 34, 7160−7169

the reactor was packed with catalyst in accordance with an in-house reactor packing scheme. The reaction zone occupying the middle segment of the reactor contained 20 mL of catalyst pellets, mixed with another 20 mL of 20/30 mesh size glass beads to help minimize wall effects and back mixing. The space on top of and below the reaction zone was filled with layers of inert packing material of variable size. The function of this material was to promote distribution of reactants. Thermocouples were inserted in both ends of the reactor for temperature monitoring and control. The reactor was configured to operate in upflow mode to optimize catalyst bed wetting.

2.2.2. Catalyst Activation and Stabilization. The hydrotreating and hydrocracking catalysts used to execute the first and second phases of the test plan, respectively, were activated in situ by following different procedures. The hydrotreating catalyst was sulfided in the liquid phase with a flow of light gas oil spiked with 3 wt % dimethyl disulfide, whereas the hydrocracking catalyst was activated in the gas phase by using hydrogen with 3 vol % hydrogen sulfide (H_2S). Following activation, the fresh catalysts were stabilized by exposing them to hydrocarbon feed for 7 days. Stabilization of the hydrotreating catalyst was conducted using VGO feed at reactor temperature 350 °C, liquid hourly space velocity (LHSV) 1.0 h^{-1}, pressure 9.7 MPa, and H_2/oil ratio 800 NL/L. Catalyst activity was monitored by taking daily liquid product density measurements. The hydrotreated VGO product from catalyst stabilization operations was collected and saved for use as stabilization feed for the hydrocracking catalyst in the second phase of the test program. The conditions under which the hydrocracking catalyst was stabilized were as follows: temperature, 380 °C; LHSV, 1.0 h^{-1}; pressure, 11.0 MPa; and H_2/oil ratio, 800 NL/L.

2.2.3. Co-processing Trials. After steady catalyst activity was reached in the hydrotreating phase of the test plan, the reactor temperature was increased from 350 to 365 °C and the LHSV was increased from 1.0 to 1.5 h^{-1}; VGO was still used as feed, and pressure and H_2/oil ratio were kept at 9.7 MPa and 800 NL/L, respectively. Sulfur and nitrogen contents in the liquid product were checked after 24 h of operation. Based on the initial results, the temperature had to be increased to 375 °C to achieve the desired sulfur and nitrogen contents for the hydrocracking step (<800 ppmw for sulfur and <200 ppmw for nitrogen). Once the product specifications were met, sample production was carried out over 216 catalyst h (9 days) to collect approximately 6 L of hydrotreated VGO. Subsequently, the feed was switched to the biocrude blend, keeping the same operating conditions. After a 24 h line-out period, a sample was taken for sulfur and nitrogen content analysis to confirm that the hydrotreated biocrude blend met the required specifications at the set conditions. The co-processing run was then continued for another 216 catalyst h (9 days) to produce about 6 L of hydrotreated biocrude blend. During the production runs, hydrotreated liquid products were collected daily and then washed with a 15 wt % NaOH solution in a separatory funnel to remove any dissolved H_2S and NH_3 that could impact the functioning of the hydrocracking catalyst. The NaOH solution to oil ratio used was 1:1. After the NaOH wash, the oil was washed with deionized water to remove any trace caustic. The entire hydrotreating phase lasted 826 catalyst h.

The hydrocracking phase was executed by following the scheme of operations used in the preceding phase. With the hydrocracking catalyst in steady state and hydrotreated VGO used as feed, the reaction temperature was optimized to achieve 65−75% conversion of 343 °C+ material. The resulting set of conditions from this exercise was as follows: temperature, 382 °C; LHSV, 1.5 h^{-1}; pressure, 11.0 MPa; and H_2/oil ratio, 800 NL/L. Approximately 3 L of hydrocracked VGO product was collected under such conditions over 96 h (4 days) of operation. After this, the feed was switched to hydrotreated biocrude blend, and the same operating conditions were maintained. In an analysis of the boiling point distribution of the resulting liquid product after a 24 h line-out period, a rapid drop in 343 °C+ conversion was noticed. After several iterations, the reactor temperature was adjusted to 390 °C, where the target 343 °C+ conversion was met. During this optimization effort a significant amount of hydrotreated biocrude blend was consumed, allowing collection of only 2 L of hydrocracked biocrude blend over 77 h (3 days) of operation. The hydrocracking phase was completed in 752 catalyst h. More details are provided in Results.

For both phases of the pilot test trials, 24 h mass balance runs were performed in the middle of the production runs with each feed to estimate product yields and hydrogen consumption. Based on the measurements on liquid and gas products, overall mass balance closures of more than 98.7% were obtained.

In the last phase of the test plan, fractionation of the two hydrocracked liquid products was performed in a spinning band distillation apparatus. The product samples were divided into two batches: one for distilling out naphtha (IBP−204 °C) and diesel (204−343 °C) fractions and the other for obtaining the jet fuel (180−270 °C) cut alone, as it overlaps in boiling range with naphtha and diesel.

2.2.4. Characterization of Feedstocks and Products. The bulk properties of feedstocks and products were measured using the following standard analytical methods: liquid density at 15.6 °C (ASTM D4052), simulated distillation (SimDis; ASTM D2887ext), elemental analysis C/H/N (ASTM D5291C), oxygen content by direct determination using an Elementar oxygen analyzer (in-house method), trace sulfur determination by X-ray fluorescence (ASTM D4294), trace nitrogen detection by chemiluminescence (ASTM D4629), and hydrocarbon type determination by either SARA (saturates, aromatics, resins, asphaltenes; ASTM D2007) or SAP (saturates, aromatics, polar compounds) analysis (ASTM D2007M).

Biogenic carbon content was measured in selected product samples using radiocarbon analysis (ASTM D6866). Diesel and jet fuel samples were analyzed for hydrocarbon type distributions using two-dimensional gas chromatography (GC×GC) with a flame ionization detector (GC×GC-FID). The GC×GC instrument comprised an Agilent 6890 gas chromatograph with a split/splitless injector, a Leco Instruments liquid-nitrogen-cooled quad-jet cryogenic modulator, and an Agilent Sievers sulfur chemiluminescence detector (Agilent Technologies, Inc., Santa Clara, CA) operating in tandem with an Agilent FID. The columns used for the analyses were an Agilent VF-5ht (29.5 m × 0.32 mm × 0.1 μm; primary column) and an SGE Analytical Science BPX-50 (1.25 m × 0.1 mm × 0.1 μm; secondary column). The main oven temperature was initially maintained at 50 °C for 1 min, and then it was increased at a rate of 3 °C/min to 320 °C, where it was held for 1 min. The secondary oven temperature program was set up in a similar manner, but offset from the main oven by +10 °C. Method-specific parameters were as follows: inlet temperature, 340 °C; sample injection volume, 0.1 μL; split ratio, 100:1; carrier gas, helium (grade 5.3, Linde); modulator temperature, +45 °C offset from the main oven; and modulation period, 6 s.

Naphtha samples were analyzed by PIONA (paraffin, isoparaffin, olefins, naphthenes, aromatics) analysis (ASTM D8071) using a GC-VUV (gas chromatography with vacuum ultraviolet detector; VUV Analytics, Inc., Cedar Park, TX) instrument. The GC-VUV instrument consisted of an Agilent 7890 gas chromatograph equipped with an Agilent 7683 autosampler and a VGA-101 VUV detector. Separation conditions were as follows: Restek Rxi-1 ms column (30 m × 0.25 mm × 0.25 μm); injector, 270 °C; split ratio, 300:1; injection volume, 1 μL; carrier gas, helium (grade 5.3, Linde); flow rate, 1.0 mL/min (constant); oven program, 30 °C for 10 min, ramped at 7 °C/min to 200 °C. The detector transfer line and flow cell were kept at 270 °C, the makeup gas was nitrogen, and makeup gas pressure was 0.25 psi. GC-VUV data were analyzed using VGA-101 software (VUV Analytics, Inc.).

3. RESULTS AND DISCUSSION

3.1. Hydrotreating. The bulk properties of the two feedstocks going into the hydrotreating process are listed in Table 1. The most marked difference between the reference VGO and biocrude blend is that the latter contains 1.4 wt % oxygen, as a result of adding the HTL biocrude distillate with 10.9 wt % oxygen. Other visible characteristics of the biocrude blend are that it is higher in polars and shows slightly more low

https://dx.doi.org/10.1021/acs.energyfuels.0c00937
Energy Fuels 2020, 34, 7160−7169

Table 1. Properties of VGO and Biocrude Blend[a]

property	VGO	biocrude blend
density at 15.6 °C, g/cm^3	0.9752	0.9751
carbon, wt %	84.7	84.0
hydrogen, wt %	11.5	11.2
sulfur, wt %	3.3	3.2
nitrogen, wt %	0.2	0.2
oxygen, wt %	0.5	1.4
SARA analysis		
saturates, wt %	37.1	36.4
aromatics, wt %	51.0	46.9
polars, wt %	11.9	16.7
n-C_5 insolubles, wt %	0.0	0.0
simulated distillation		
IBP, °C	293.6	198.2
5 wt %, °C	342.8	323.4
10 wt %, °C	361.6	351.8
30 wt %, °C	404.6	399.0
50 wt %, °C	434.4	432.0
70 wt %, °C	466.2	464.8
80 wt %, °C	486.0	485.6
90 wt %, °C	515.4	516.4
95 wt %, °C	555.8	557.8
FBP, °C	—	—

[a]IBP, initial boiling point; FBP, final boiling point; SARA, saturates, aromatics, resins, asphaltenes; VGO, vacuum gas oil.

boiling fractions (<343 °C) than VGO. It should be noted that the elemental composition in some case does not add up to exactly 100% due to measurement error.

Figure 2 shows the hydrodesulfurization (HDS) and hydrodenitrogenation (HDN) performances during the hydrotreating phase of the program. On average, HDS and HDN for the reference VGO feed were maintained at 99.4% and 97.7%, respectively. After the biocrude blend was introduced at 578 catalyst h, HDN activity was observed to slightly decrease by ~4%, while the impact on HDS was marginal. This behavior is consistent with our previous study[36] showing that HDS is not significantly affected at co-processing ratios below 10 vol % and temperatures of 370 °C and above.

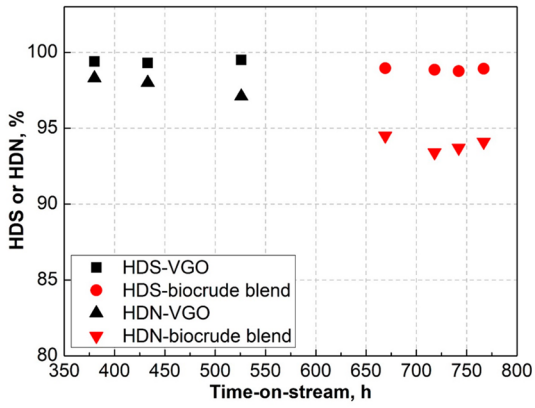

Figure 2. Monitoring of catalyst performance during the hydrotreating phase.

The properties of the total liquid products resulting from the hydrotreating step are listed in Table 2. The two hydrotreated (HT) products, hereafter referred to as HT-VGO and HT-biocrude blend, are very similar in liquid density (0.9020 g/cm^3 for HT-VGO vs 0.9025 g/cm^3 for HT-biocrude blend) and satisfy the prescribed sulfur (<800 ppmw sulfur) and nitrogen (<200 ppmw nitrogen) content limits for the subsequent hydrocracking step. A noticeable difference, nevertheless, is the oxygen content of the two products. The fact that HT-biocrude blend has 1530 ppmw oxygen is an indication that the hydrotreating catalyst is not as effective in removing oxygen compounds in HTL biocrude as it is in removing sulfur and nitrogen from petroleum. Oxygen content in the product also had repercussions on the hydrocracking step, which is analyzed in section 3.2. Hydrotreating also creates a shift in boiling point distribution, resulting in 28.4–29.7 wt % light material boiling below 343 °C. In terms of hydrocarbon type composition, hydrotreating reduces polars and aromatics content to 2.6–2.9 and 33.6–35.6 wt %, respectively, while increasing the share of saturates to 61.8–63.5 wt %.

Table 2. Properties of the Total Liquid Products from the Hydrotreating (HT) Step[a]

property	HT-VGO	HT-biocrude blend
density at 15.6 °C, g/cm^3	0.9020	0.9025
sulfur, ppmw	200	410
nitrogen, ppmw	46	92
oxygen, ppmw	<1000[b]	1530
IBP–343 °C, wt %	28.4	29.7
SAP analysis		
saturates, wt %	61.8	63.5
aromatics, wt %	35.6	33.6
polars, wt %	2.6	2.9

[a]IBP, initial boiling point; SAP, saturates, aromatics, polar compounds; VGO, vacuum gas oil. [b]Value below the 1000 ppmw detection limit of the oxygen analyzer.

Product yields and other process performance parameters estimated from the mass balance runs are reported in Table 3. As observed, hydrotreating the VGO and biocrude blend generates a similar product yield structure, with a total liquid

Table 3. Product Yields and Catalytic Performance during the Hydrotreating (HT) Step[a]

parameter	VGO	biocrude blend
operating conditions		
average temperature, °C	375	374
LHSV, h^{-1}	1.5	1.5
pressure, MPa	9.7	9.7
H_2/oil ratio, NL/L	800	800
product distribution		
light end (C_1–C_4), wt %	0.6	0.7
H_2S, wt %	3.5	3.4
naphtha (IBP–204 °C), wt %	5.4	6.1
light gas oil (204–343 °C), wt %	20.1	20.7
vacuum gas oil (343 °C+), wt %	72.1	70.8
total, wt %	101.7	101.7
liquid product yield, wt %	97.6	97.6
catalytic performance		
hydrodesulfurization, %	99.5	98.9
hydrodenitrogenation, %	97.2	93.6
hydrodeoxygenation, %	>81.2	89.2
hydrogen consumption, scf/bbl	1074	1099

[a]IBP, initial boiling point; LHSV, liquid hourly space velocity; VGO, vacuum gas oil.

https://dx.doi.org/10.1021/acs.energyfuels.0c00937
Energy Fuels 2020, 34, 7160–7169

product yield of 97.6 wt %. VGO generates slightly more H_2S (3.5 wt %) than the biocrude blend (3.4 wt %) as a result of the differences in HDS levels between the two feedstocks (99.5% for VGO vs 98.9% for the biocrude blend). To a small extent, the biocrude blend shows higher light end yield (0.7 wt %) than VGO (0.6 wt %), likely due to oxygen removal reactions leading to carbon monoxide and carbon dioxide. HT-biocrude blend is somewhat higher in naphtha (6.1 wt %) and light gas oil (20.7 wt %) fractions than HT-VGO, owing to the fact that the biocrude blend initially had 8.0 wt % distillates boiling below 343 °C while VGO had 5 wt % of such material (see Table 1). Hydrogen consumption calculations based on an overall hydrogen balance in the gas and liquid phases show quite comparable levels for hydrotreating of VGO (1074 scf/bbl) and biocrude blend (1099 scf/bbl). This is in line with what was concluded in our previous work regarding hydrogen consumption during HTL biocrude co-processing.[36]

3.2. Hydrocracking. Figure 3 depicts the catalyst activity profile during the hydrocracking phase using HT-VGO and

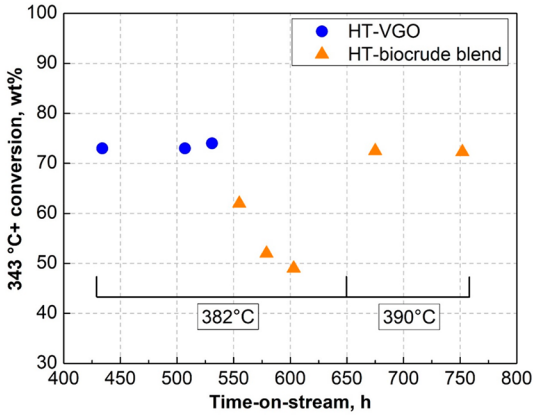

Figure 3. Monitoring of catalyst performance during the hydrocracking phase.

HT-biocrude blend as feedstocks. Catalyst activity was monitored in terms of the conversion of 343 °C+ material in the feed, which was estimated from the boiling point distribution of the hydrocracked products. As mentioned in the Experimental Section, reaction temperature during this testing phase was set through an optimization exercise with the goal of achieving 343 °C+ conversion levels of 65.0−75.0%. In the case of HT-VGO, a reactor temperature of 382 °C enabled attainment of 73.2% 343 °C+ conversion. This level of conversion was maintained fairly constant over the production run with HT-VGO, as shown in Figure 3.

Also shown in Figure 3 is that, on switching the feed from HT-VGO to HT-biocrude blend at nearly 550 catalyst h and keeping the temperature at 382 °C, 343 °C+ conversion declined rapidly to under 50.0% in about 50 h of operation. A similar kind of catalyst deactivation during hydrotreating of pyrolysis oil and HTL biocrude, which contains higher amounts of oxygen, has been reported.[37,38] According to properties of the hydrotreated products presented in Table 2, there was strong indication that oxygen content in HT-biocrude blend was the major cause of this behavior. Table 2 also shows that HT-biocrude blend contains more nitrogen (92 ppmw) than HT-VGO (46 ppmw), which could have also contributed to this behavior, as nitrogen compounds are known to have an inhibitory effect on hydrocracking catalysts.[39,40] Our hypothesis is that the oxygen and nitrogen compounds in the biocrude blend that persisted after hydrotreating inhibit the function of the hydrocracking catalyst. To address this problem, further adjustments in temperature were made to be able to match the 343 °C+ conversion obtained for HT-VGO. This mitigation led to increasing the reactor temperature from 382 to 390 °C to achieve and maintain ~72.5% 343 °C+ conversion throughout the production run with HT-biocrude blend.

Table 4 reports the bulk properties of the hydrocracked (HC) liquid products, hereafter referred to as HC-VGO and

Table 4. Properties of the Total Liquid Products from the Hydrocracking (HC) Step[a]

property	HC-VGO	HC-biocrude blend
density at 15.6 °C, g/cm^3	0.8071	0.8108
sulfur, ppmw	145	50
nitrogen, ppmw	0.4	1.2
oxygen, ppmw	<1000[b]	<1000[b]
IBP−343 °C, wt %	80.6	80.5

[a]IBP, initial boiling point; VGO, vacuum gas oil. [b]Value below the 1000 ppmw detection limit of the oxygen analyzer.

HC-biocrude blend. The two products contained trace amounts of nitrogen (0.4 ppmw for HC-VGO vs 1.2 ppmw of HC-biocrude blend), yet sulfur content was still visible (145 ppmw for HC-VGO vs 50 ppmw for HC-biocrude blend). The larger extent of sulfur removal observed for HC-biocrude blend is attributed to using a reaction temperature that was 8 °C higher for hydrocracking HT-biocrude blend. The yield of IBP−343 °C distillate fractions in the hydrocracked products was 80.5−80.6 wt %. Figure 4 illustrates in detail the changes in boiling point distribution of the starting feedstocks and their products after they were subjected to hydrotreating and hydrocracking.

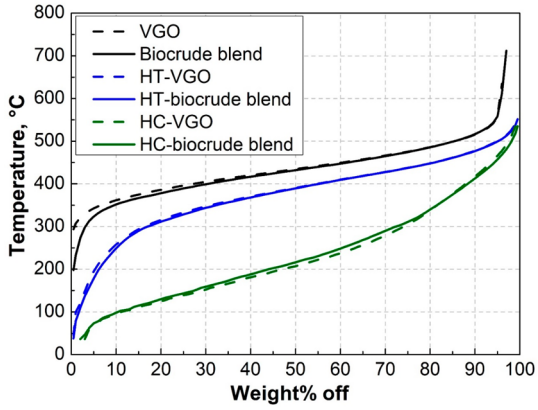

Figure 4. Boiling point distribution for the starting feedstocks and their products after hydrotreating and hydrocracking.

Product yield, conversion, and hydrogen consumption calculated for the hydrocracking step are given in Table 5. All calculated values are reported on a hydrotreated feed basis. With similar 343 °C+ conversion levels, hydrocracking of HT-VGO and HT-biocrude blend leads to similar results for yield structure and for hydrogen consumption. Light end production is in the 2.8−3.0 wt % range, while H_2S yield is negligible, as most of the sulfur was removed during hydrotreating. HT-

https://dx.doi.org/10.1021/acs.energyfuels.0c00937
Energy Fuels 2020, 34, 7160−7169

Table 5. Product Yields and Catalytic Performance during the Hydrocracking (HC) Step[a]

parameter	HT-VGO	HT-biocrude blend
operating conditions		
average temperature, °C	382	390
LHSV, h^{-1}	1.5	1.5
pressure, MPa	11.0	11.0
H_2/oil ratio, NL/L	800	800
product distribution		
light end (C_1–C_4), wt %	3.0	2.8
H_2S, wt %	0.0	0.0
naphtha (IBP–204 °C), wt %	49.8	45.9
diesel (204–343 °C), wt %	31.1	33.6
unconverted oil (343 °C+), wt %	18.1	19.6
total, wt %	102.0	101.9
liquid product yield, wt %	99.0	99.1
catalytic performance		
343 °C+ conversion, wt %	73.2	72.5
hydrogen consumption, scf/bbl	1202	1149

[a]IBP, initial boiling point; LHSV, liquid hourly space velocity; VGO, vacuum gas oil.

VGO yields 3.9 wt % more naphtha fraction than HT-biocrude blend, but 2.5 wt % less diesel fraction. Hydrogen consumption for this step was estimated at 1202 scf/bbl for HT-VGO and 1149 scf/bbl for HT-biocrude blend. It should be noted that the yields of liquid fractions are not from physical distillation, but are from the simulated distillation data shown in Figure 4. Results of the physical distillation of hydrocracked products are discussed in section 3.3.

The overall product distribution and hydrogen consumption of the combined hydrotreating–hydrocracking process are compared for each feedstock in Table 6. All values are on a starting feed basis, that is, either VGO or biocrude blend. Despite the fact that the co-processing scheme required a higher temperature during the hydrocracking step to manage the oxygen content problem in HT-biocrude blend, this scheme in general is very close to the VGO baseline values for product yields and hydrogen consumption. As such, these results hold promise and point to areas needing further research, the most evident one being oxygen removal in biocrude to improve co-processing efficiency in the hydrocracking step.

Table 6. Overall Product Distribution and Hydrogen Consumption[a]

parameter	VGO	biocrude blend
light end (C_1–C_4), wt %	3.5	3.5
H_2S, wt %	3.5	3.4
naphtha (IBP–204 °C), wt %	48.6	44.8
diesel (204–343 °C), wt %	30.3	32.8
unconverted oil (343 °C+), wt %	17.7	19.1
total, wt %	103.6	103.6
hydrogen consumption, scf/bbl	2343	2310

[a]IBP, initial boiling point; VGO, vacuum gas oil.

3.3. Bulk Property Characterization of Distillation Fractions. Hydrocracked liquid products from VGO and the biocrude blend were physically fractionated into naphtha, diesel, and jet fuel. The distillation yields and bulk properties of these fractions are compared in Table 7. The yields of jet fuel fraction (180–270 °C), which were not reported in the previous section, were 27.0 wt % for HC-VGO and 25.7 wt % for HC-biocrude blend. There are subtle differences in bulk properties between the fractions from HC-VGO and HC-biocrude blend. The naphtha fraction from HC-biocrude blend has a lower sulfur content (1 ppmw) than that from HC-VGO (33 ppmw), most likely due to the fact that a higher hydrocracking temperature was used for HC-biocrude blend. A similar conclusion applies to the jet fuel fraction. Sulfur content in the diesel fractions, on the other hand, is virtually identical (75–78 ppmw). Boiling point distribution curves depicted in Figure 5 show negligible differences between the fractions from HC-VGO and HC-biocrude blend.

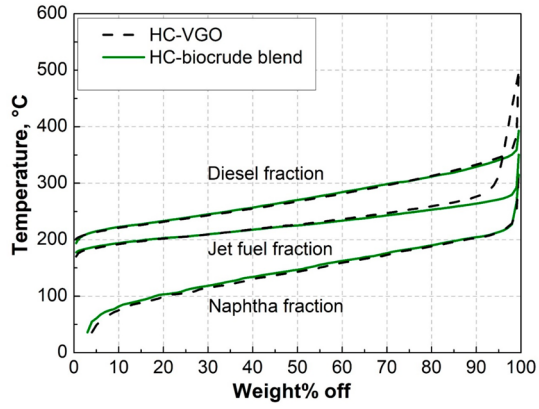

Figure 5. Boiling point distribution for the naphtha, diesel, and jet fuel fractions resulting from the distillation of hydrocracked liquid products.

Table 7. Distillation Yields and Bulk Properties of the Naphtha, Diesel, and Jet Fuel Fractions Resulting from the Distillation of Hydrocracked (HC) Liquid Products[a]

	HC-VGO			HC-biocrude blend		
property	naphtha	diesel	jet fuel	naphtha	diesel	jet fuel
yield, wt %	52.3	29.3	27.0	46.3	31.1	25.7
density at 15.6 °C, g/cm^3	0.7661	0.8515	0.8408	0.7734	0.8522	0.8443
carbon, wt %	84.8	86.9	86.4	84.2	86.6	86.6
hydrogen, wt %	14.0	13.3	13.2	13.8	13.2	13.0
sulfur, ppmw	33	78	29	1	75	10
nitrogen, ppmw	<1	<1	<1	<1	<1	<1

[a]VGO, vacuum gas oil.

https://dx.doi.org/10.1021/acs.energyfuels.0c00937
Energy Fuels 2020, 34, 7160–7169

3.4. Hydrocarbon Type Characterization of Distillation Fractions.

Table 8 shows the hydrocarbon type composition of the distillation fractions from the two hydrocracked products. As mentioned in the Experimental Section, hydrocarbon typing in naphtha was carried out using a GC-VUV instrument, while diesel and jet fuel fractions were characterized by GC×GC-FID. Olefins are reported only for naphtha, as GC×GC-FID is unable to detect olefins because of their strong coelution with cycloparaffins. It is observed that all distillation products are predominantly cycloparaffinic (>49.5 wt %) as a result of the hydrogenation of the abundant aromatic compounds in both VGO and HTL biocrude. The fractions from HC-biocrude blend are higher in aromatics (alkylbenzenes, tetralins, and diaromatics) than those from HC-VGO. For example, indans/tetralins content in the diesel and jet fuel fractions from HC-biocrude stands at 12.3 and 15.1 wt %, respectively, whereas in the corresponding fractions from HC-VGO indans/tetralins account for 11.0 and 12.4 wt %, respectively. The increased presence of aromatics in co-processed products is indicative of the contribution of the various oxygenated aromatic species in HTL biocrude.[30] Also

Table 8. Hydrocarbon Type Composition of Distillation Fractions[a]

	HC-VGO			HC-biocrude blend		
hydrocarbon class	naphtha	diesel	jet fuel	naphtha	diesel	jet fuel
n-paraffins, wt %	6.4	2.9	2.5	5.9	6.5	2.9
isoparaffins, wt %	31.4	15.7	14.4	27.3	15.1	12.8
cycloparaffins, wt %	49.5	57.8	58.3	52.2	52.5	56.0
alkylbenzenes, wt %	10.6	10.0	11.7	11.9	10.4	12.4
indans/tetralins, wt %	0.0	11.0	12.4	0.0	12.3	15.1
diaromatics, wt %	0.0	2.5	0.7	0.0	3.1	0.8
triaromatics, wt %	0.0	0.1	0.0	0.0	0.1	0.0
olefins, wt %	2.1	–	–	2.7	–	–

[a]HC, hydrocracked; VGO, vacuum gas oil.

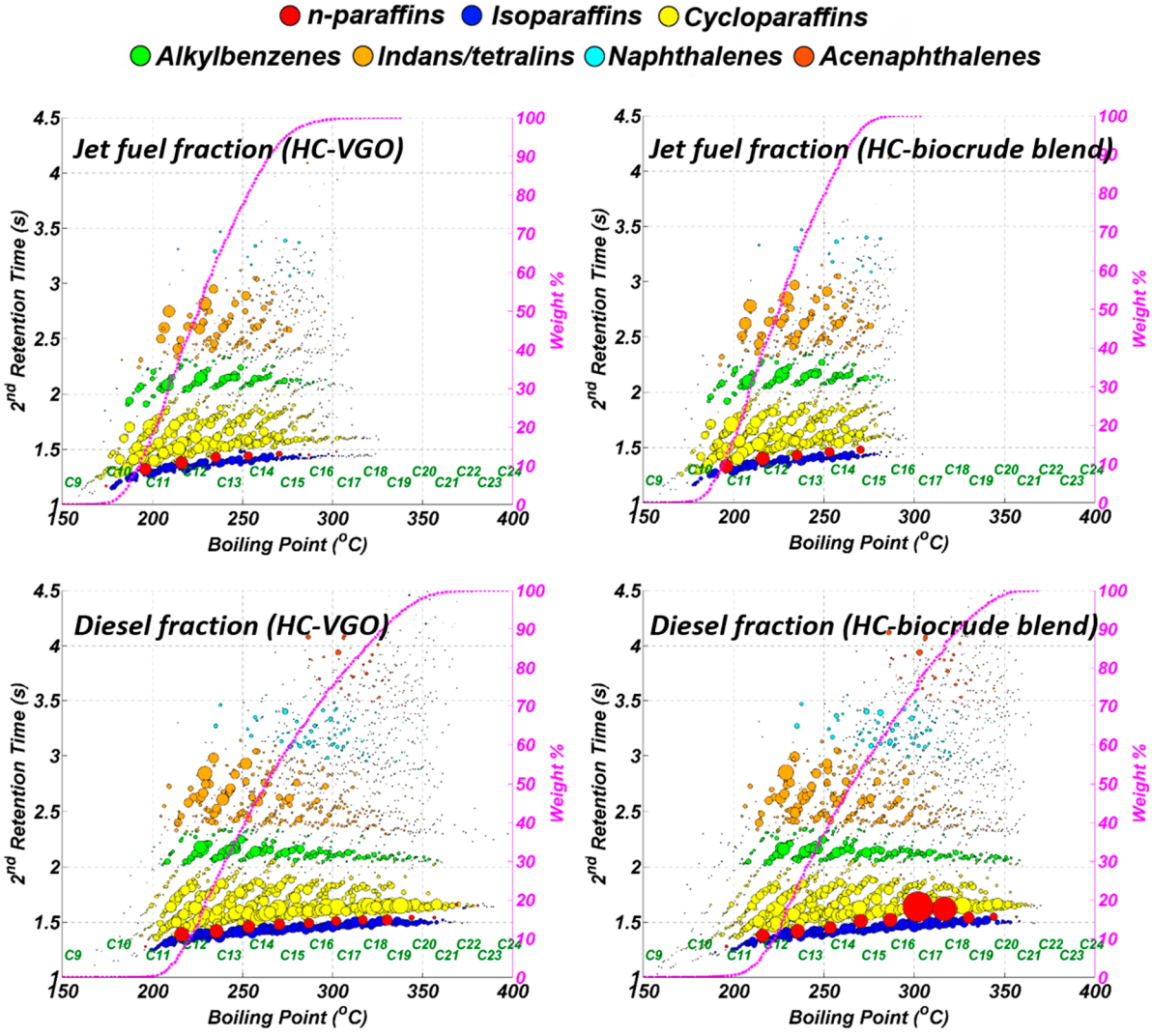

Figure 6. Bubble plot representation of "normal" GC×GC-FID contour plots of jet fuel and diesel fractions from HC-VGO and HC-biocrude blend. The bubble size and color are related to the compound concentration and hydrocarbon type, respectively. Green labels at the bottom of each plot indicate the positions of *n*-paraffins. The magenta line depicts the SimDis curve calculated on the basis of GC×GC data. GC×GC, two-dimensional gas chromatography; FID, flame ionization detector; HC, hydrocracked; VGO, vacuum gas oil.

https://dx.doi.org/10.1021/acs.energyfuels.0c00937
Energy Fuels 2020, 34, 7160−7169

noted is that the diesel fraction from HC-biocrude blend is higher in *n*-paraffins (6.5 wt %) than that of HC-VGO (2.9 wt %). The extra *n*-paraffins in the co-processed diesel fraction are likely to originate from fatty acid compounds that have been previously identified in HTL biocrude.[36,41]

Figure 6 is a bubble plot representation of the GC×GC-FID chromatograms for the diesel and jet fuel fractions. The bubble plot format presents hydrocarbon types as series of color-coded bubbles, where each specific color represents one hydrocarbon class and the size of each colored bubble is proportional to the mass fraction of the compound. Given their level of detail, these bubble plots serve as compositional fingerprints for visual comparison of hydrocarbon samples. From Figure 6 it is clearly seen that the jet fuel samples on the top panel significantly differ from the diesel samples on the bottom panel, but differences between the diesel and jet fuel fractions from HC-VGO and the corresponding fractions from HC-biocrude blend are not evident. The only visible variation is attributed to the two large red bubbles representing *n*-heptadecane (*n*-C_{17}) and *n*-octadecane (*n*-C_{18}) in the co-processed diesel fraction. These two compounds constitute the additional *n*-paraffins noted in Table 8. Based on previous evidence, we believe these compounds derive from C_{17}−C_{18} fatty acids originally present in HTL biocrude.[36,41] Very subtle differences in concentration can also be found near the final boiling point region of each fraction, which is around 270 °C for the jet fuel fraction and 343 °C for the diesel fraction. These differences are most probably caused by batch-to-batch variability in the physical distillation process to obtain these fractions.

3.5. Biogenic Carbon Distribution in Co-processed Products. Radiocarbon measurements were conducted to understand the fate of biogenic carbon during co-processing. Table 9 reports the biogenic carbon contents in the starting biocrude blend and its intermediate and final products. Analytical measurements are reported as a percentage of modern carbon (second column), which are then converted to biogenic carbon content relative to the total amount of carbon in the sample (third column) by rounding up or down the measured values to the nearest whole number as per the testing standard (ASTM D6866). For instance, if the modern carbon is 5.50−6.49%, the biogenic carbon content is 6%. It is important to point out that the ASTM D6866 method assigns a ±3% absolute error to the resulting biogenic carbon content values. The last column shows the biogenic carbon per 100 g of feed (biocrude blend), which is calculated on the basis of the biogenic carbon contents in the third column and total carbon contents in the feed and co-processed products. The results from this last column are used for tracking the distribution of biogenic carbon throughout the process on a starting feed basis.

Table 9. Biogenic Carbon Content in Co-processed Products[a]

sample	modern carbon (%)	biogenic carbon (%)	biogenic carbon (g/100 g of feed)
biocrude blend	7.51	8	6.7
HT-biocrude blend	7.25	7	5.8
HC-biocrude blend	7.47	7	5.8
naphtha fraction	8.39	8	3.0
diesel fraction	10.29	10	2.6
343 °C+ fraction	0.90	1	0.2
jet fuel fraction	7.51	8	1.7

[a]HC, hydrocracked; HT, hydrotreated.

The measured biogenic carbon percentage in the biocrude blend (8%) is noted to be very similar to the ratio of HTL biocrude distillate in the feed (7.5 vol %). Based on our calculation in the last column of Table 9, the feed-based biogenic carbon content in the biocrude blend corresponds to 6.7 g/100 g of feed. After hydrotreating, this value decreases to 5.8 g/100 g of feed, implying a 13.4% loss in biogenic carbon during this step of the process. Biogenic carbon loss to gas can certainly be expected during hydrotreating, but the magnitude of such loss should be much smaller considering the light end yields presented in Table 3. More than an actual carbon loss during the process, this is a calculation error resulting from rounding modern carbon values to obtain biogenic carbon contents. Modern carbon results for the biocrude blend (7.51%) and HT-biocrude blend (7.25%) in fact are very close; however, after rounding these values, a 1% gap in biogenic carbon content is created between these two streams, thus revealing another limitation of the testing method apart from the ±3% error margin. The feed-based biogenic carbon content in the total product of the hydrocracking step (5.8 g/100 g of feed) would suggest no losses in biogenic carbon during this step of the process.

The biogenic carbon content in the co-processed naphtha, diesel, and jet fuel fractions is found to be in the 8−10% range. The feed-based biogenic carbon calculations for naphtha (3.0 g/100 g of feed) and diesel (2.6 g/100 g of feed) indicate that 96.5% of the biogenic carbon entering the hydrocracking step (5.8 g/100 g of feed) is retained in the naphtha and diesel fractions, with the rest remaining in the unconverted 343 °C+ fraction. In a jet fuel production scenario, the jet fuel fraction (1.7 g/100 g of feed) would capture 29.3% of the biogenic carbon in the hydrocracker feed. Thus, it is suggested that co-processing HTL biocrude in a hydrocracking process not only can maintain product yields and quality near baseline levels, but also can achieve a favorable biogenic carbon distribution in the final fuel products.

4. CONCLUSIONS

We have demonstrated the potential of co-processing HTL biocrude with VGO by using a hydrocracking process with a preparatory hydrotreating step. The conclusions of this study are as follows:

- Hydrotreating achieved the required sulfur and nitrogen removal levels in the biocrude blend to meet the specifications of the hydrocracking catalyst. However, the hydrotreating process was not as effective in removing oxygen compounds in HTL biocrude, which resulted in a hydrotreated product having 1530 ppmw oxygen.
- To achieve ∼73.0% 343 °C+ conversion in the hydrocracking step, the hydrotreated biocrude blend required 8 °C more in reaction temperature. We attribute this behavior to catalyst inhibition effects by oxygen and nitrogen compounds in the biocrude blend that persisted after hydrotreating.
- The overall product distribution and hydrogen consumption for the hydrotreating−hydrocracking of the biocrude

https://dx.doi.org/10.1021/acs.energyfuels.0c00937
Energy Fuels 2020, 34, 7160−7169

blend were very similar to the baseline values observed for VGO.

- The co-processed naphtha, diesel, and jet fuel fractions showed minor differences in bulk properties with respect to those from pure VGO.
- Hydrocarbon type characterization showed that the co-processed fractions are slightly higher in aromatic compounds. The co-processed diesel fraction was also found to be more paraffinic. Aromatic oxygen compounds and fatty acids in HTL biocrude are likely to be the source of these additional aromatic and paraffinic compounds.
- The co-processed fractions had 8−10% biogenic carbon contents. Based on our calculations, the naphtha, diesel, and jet fuel fractions retained 51.7, 44.8, and 29.3%, respectively, of the biogenic carbon entering the hydrocracking step.

AUTHOR INFORMATION

Corresponding Author

Anton Alvarez-Majmutov − *CanmetENERGY Devon, Natural Resources Canada, Devon, Alberta, Canada T9G 1A8;* orcid.org/0000-0002-6958-3959; Phone: (+1) 780-987-8348; Email: anton.alvarez-majmutov@canada.ca; Fax: (+1) 780-987-5349

Authors

Sandeep Badoga − *CanmetENERGY Devon, Natural Resources Canada, Devon, Alberta, Canada T9G 1A8*

Tingyong Xing − *CanmetENERGY Devon, Natural Resources Canada, Devon, Alberta, Canada T9G 1A8*

Rafal Gieleciak − *CanmetENERGY Devon, Natural Resources Canada, Devon, Alberta, Canada T9G 1A8;* orcid.org/0000-0002-5409-3498

Jinwen Chen − *CanmetENERGY Devon, Natural Resources Canada, Devon, Alberta, Canada T9G 1A8*

Complete contact information is available at: https://pubs.acs.org/10.1021/acs.energyfuels.0c00937

Notes

The authors declare no competing financial interest.

ACKNOWLEDGMENTS

Funding for this study was provided by the Government of Canada's Forest Innovation Program (FIP). The authors would like to thank the pilot plant and analytical lab staff at CanmetENERGY Devon for their technical support. Comments from Dr. Rahman Gholami on revising the manuscript are greatly appreciated. The authors are grateful to Steeper Energy for kindly supplying the HTL biocrude sample used in this study.

REFERENCES

(1) Lane, J. *Biofuels Mandates Around the World 2018*. Biofuels Digest. January 1, 2018. https://www.biofuelsdigest.com/bdigest/2018/01/01/biofuels-mandates-around-the-world-2018/.

(2) DOE. *Altrenative Fuels Data Center*. https://afdc.energy.gov/fuels/biodiesel_blends.html.

(3) Natural Resources Canada. *Renewable Energy Facts*. https://www.nrcan.gc.ca/energy/facts/renewable-energy/20069#L8 (accessed 2020-01-25).

(4) Mohan, D.; Pittman, C. U.; Steele, P. H. Pyrolysis of Wood/Biomass for Bio-Oil: A Critical Review. *Energy Fuels* **2006**, *20* (3), 848−889.

(5) Hawash, S. I.; Farah, J. Y.; El-Diwani, G. Pyrolysis of Agriculture Wastes for Bio-Oil and Char Production. *J. Anal. Appl. Pyrolysis* **2017**, *124*, 369−372.

(6) Sipra, A. T.; Gao, N.; Sarwar, H. Municipal Solid Waste (MSW) Pyrolysis for Bio-Fuel Production: A Review of Effects of MSW Components and Catalysts. *Fuel Process. Technol.* **2018**, *175*, 131−147.

(7) Jensen, C. U.; Rodriguez Guerrero, J. K.; Karatzos, S.; Olofsson, G.; Iversen, S. B. Fundamentals of Hydrofaction ™: Renewable Crude Oil from Woody Biomass. *Biomass Convers. Biorefin.* **2017**, *7* (4), 495−509.

(8) Gollakota, A. R.; Kishore, N.; Gu, S. A Review on Hydrothermal Liquefaction of Biomass. *Renewable Sustainable Energy Rev.* **2018**, *81*, 1378−1392.

(9) Ouadi, M.; Jaeger, N.; Greenhalf, C.; Santos, J.; Conti, R.; Hornung, A. Thermo-Catalytic Reforming of Municipal Solid Waste. *Waste Manage.* **2017**, *68* (2017), 198−206.

(10) Mandal, S.; Bandyopadhyay, R.; Das, A. K. Thermo-Catalytic Process for Conversion of Lignocellulosic Biomass to Fuels and Chemicals: A Review. *Int. J. Petrochemical Sci. Eng.* **2018**, *3* (2), 78−89.

(11) van Dyk, S.; Su, J.; Mcmillan, J. D.; Saddler, J. Potential Synergies of Drop-in Biofuel Production with Further Co-Processing at Oil Refineries. *Biofuels, Bioprod. Biorefin.* **2019**, *13* (3), 760−775.

(12) Bezergianni, S.; Dimitriadis, A.; Kikhtyanin, O.; Kubička, D. Refinery Co-Processing of Renewable Feeds. *Prog. Energy Combust. Sci.* **2018**, *68*, 29−64.

(13) Al-Sabawi, M.; Chen, J.; Ng, S. Fluid Catalytic Cracking of Biomass-Derived Oils and Their Blends with Petroleum Feedstocks: A Review. *Energy Fuels* **2012**, *26* (9), 5355−5372.

(14) Furimsky, E. Hydroprocessing Challenges in Biofuels Production. *Catal. Today* **2013**, *217*, 13−56.

(15) Al-Sabawi, M.; Chen, J. Hydroprocessing of Biomass-Derived Oils and Their Blends with Petroleum Feedstocks: A Review. *Energy Fuels* **2012**, *26* (9), 5373−5399.

(16) Egeberg, R.; Knudsen, K.; Nyström, S.; Grennfelt, E. L.; Efraimsson, K. Industrial-scale production of renewable diesel. *Petroleum Technology Quarterly* **2011**, *Q3*, 59−65.

(17) Chum, H. L.; Pinho, A.; Freel, B. Presented at the DOE Bioenergy Technologies Office (BETO) 2015 Project Peer Review; Alexandria, VA, USA.

(18) Parkland Fuel Corp. *Burnaby Coprocessing Opportunity*. http://www.parklandcap.ca/wp/wp-content/uploads/2018/10/Attachment-Two_CAP_BC_Biofuel-Opportunity_May16_2018.pdf.

(19) *Advanced Biofuels: Hydrotreated Vegetable Oils-Coprocessing*. https://www.eafo.eu/alternative-fuels/advanced-biofuels/hvo (accessed 2020-01-25).

(20) Eschenbacher, A.; Myrstad, T.; Bech, N.; Duus, J. Ø.; Li, C.; Jensen, P. A.; Henriksen, U. B.; Ahrenfeldt, J.; Mentzel, U. V.; Jensen, A. D. Co-Processing of Wood and Wheat Straw Derived Pyrolysis Oils with FCC Feed—Product Distribution and Effect of Deoxygenation. *Fuel* **2020**, *260*, 116312.

(21) Stefanidis, S. D.; Kalogiannis, K. G.; Lappas, A. A. Co-Processing Bio-Oil in the Refinery for Drop-in Biofuels via Fluid Catalytic Cracking. *Wiley Interdiscip. Rev.: Energy Environ.* **2018**, *7* (3), e281.

(22) Pinheiro Pires, A. P.; Arauzo, J.; Fonts, I.; Domine, M. E.; Fernández Arroyo, A.; Garcia-Perez, M. E.; Montoya, J.; Chejne, F.; Pfromm, P.; Garcia-Perez, M. Challenges and Opportunities for Bio-Oil Refining: A Review. *Energy Fuels* **2019**, *33* (6), 4683−4720.

(23) de Miguel Mercader, F.; Groeneveld, M. J.; Kersten, S. R. A.; Way, N. W. J.; Schaverien, C. J.; Hogendoorn, J. A. Production of Advanced Biofuels: Co-Processing of Upgraded Pyrolysis Oil in Standard Refinery Units. *Appl. Catal., B* **2010**, *96* (1−2), 57−66.

(24) French, R. J.; Stunkel, J.; Baldwin, R. M. Mild Hydrotreating of Bio-Oil: Effect of Reaction Severity and Fate of Oxygenated Species. *Energy Fuels* **2011**, *25* (7), 3266−3274.

(25) Gueudré, L.; Chapon, F.; Mirodatos, C.; Schuurman, Y.; Venderbosch, R.; Jordan, E.; Wellach, S.; Gutierrez, R. M. Optimizing

the Bio-Gasoline Quantity and Quality in Fluid Catalytic Cracking Co-Refining. *Fuel* **2017**, *192*, 60−70.
(26) Fogassy, G.; Thegarid, N.; Toussaint, G.; van Veen, A. C.; Schuurman, Y.; Mirodatos, C. Biomass Derived Feedstock Co-Processing with Vacuum Gas Oil for Second-Generation Fuel Production in FCC Units. *Appl. Catal., B* **2010**, *96* (3−4), 476−485.
(27) Mortensen, P. M.; Grunwaldt, J. D.; Jensen, P. A.; Knudsen, K. G.; Jensen, A. D. A Review of Catalytic Upgrading of Bio-Oil to Engine Fuels. *Appl. Catal., A* **2011**, *407* (1−2), 1−19.
(28) Elliott, D. C. Historical Developments in Hydroprocessing Bio-Oils. *Energy Fuels* **2007**, *21* (3), 1792−1815.
(29) Zacher, A. H.; Olarte, M. V.; Santosa, D. M.; Elliott, D. C.; Jones, S. B. A Review and Perspective of Recent Bio-Oil Hydrotreating Research. *Green Chem.* **2014**, *16*, 491−515.
(30) Hoffmann, J.; Jensen, C. U.; Rosendahl, L. A. Co-Processing Potential of HTL Bio-Crude at Petroleum Refineries - Part 1: Fractional Distillation and Characterization. *Fuel* **2016**, *165*, 526−535.
(31) Zhu, Y.; Biddy, M. J.; Jones, S. B.; Elliott, D. C.; Schmidt, A. J. Techno-Economic Analysis of Liquid Fuel Production from Woody Biomass via Hydrothermal Liquefaction (HTL) and Upgrading. *Appl. Energy* **2014**, *129*, 384−394.
(32) Jensen, C. U.; Hoffmann, J.; Rosendahl, L. A. Co-Processing Potential of HTL Bio-Crude at Petroleum Refineries. Part 2: A Parametric Hydrotreating Study. *Fuel* **2016**, *165*, 536−543.
(33) Ramirez, J. A.; Brown, R. J.; Rainey, T. J. Liquefaction Biocrudes and Their Petroleum Crude Blends for Processing in Conventional Distillation Units. *Fuel Process. Technol.* **2017**, *167* (May), 674−683.
(34) Mathieu, Y.; Sauvanaud, L.; Humphreys, L.; Rowlands, W.; Maschmeyer, T.; Corma, A. Opportunities in Upgrading Biomass Crudes. *Faraday Discuss.* **2017**, *197*, 389−401.
(35) Sauvanaud, L.; Mathieu, Y.; Corma, A.; Humphreys, L.; Rowlands, W.; Maschmeyer, T. Co-Processing of Lignocellulosic Biocrude with Petroleum Gas Oils. *Appl. Catal., A* **2018**, *551*, 139−145.
(36) Xing, T.; Alvarez-Majmutov, A.; Gieleciak, R.; Chen, J. Co-Hydroprocessing Biocrude from Waste Biomass with Bitumen-Derived Vacuum Gas Oil. *Energy Fuels* **2019**, *33* (11), 11135−11144.
(37) Haghighat, P.; Montanez, A.; Aguilera, G. R.; Rodriguez Guerrero, J. K.; Karatzos, S.; Clarke, M. A.; McCaffrey, W. Hydrotreating of Hydrofaction^{TM} Biocrude in the Presence of Presulfided Commercial Catalysts. *Sustain. Energy Fuels* **2019**, *3* (3), 744−759.
(38) Han, Y.; Gholizadeh, M.; Tran, C. C.; Kaliaguine, S.; Li, C. Z.; Olarte, M.; Garcia-Perez, M. Hydrotreatment of Pyrolysis Bio-Oil: A Review. *Fuel Process. Technol.* **2019**, *195*, 106140.
(39) Furimsky, E.; Massoth, F. E. Hydrodenitrogenation of Petroleum. *Catal. Rev.: Sci. Eng.* **2005**, *47* (3), 297−489.
(40) Sau, M.; Basak, K.; Manna, U.; Santra, M.; Verma, R. P. Effects of Organic Nitrogen Compounds on Hydrotreating and Hydrocracking Reactions. *Catal. Today* **2005**, *109* (1−4), 112−119.
(41) Pedersen, T. H.; Jensen, C. U.; Sandström, L.; Rosendahl, L. A. Full Characterization of Compounds Obtained from Fractional Distillation and Upgrading of a HTL Biocrude. *Appl. Energy* **2017**, *202*, 408−419.

https://dx.doi.org/10.1021/acs.energyfuels.0c00937
Energy Fuels 2020, 34, 7160−7169